The Abdus Salam International Centre for Theoretical Physics

United Nations Educational, Scientific and Cultural Organization

IAEA International Atomic Energy Agency

2048-9

From Core to Crust: Towards an Integrated Vision of Earth's Interior

20 - 24 July 2009

Computing deep Earth structure

G. Steinle-Neumann
Universitat Bayreuth, Germany

Computing deep Earth structure
The role of potassium in the deep Earth

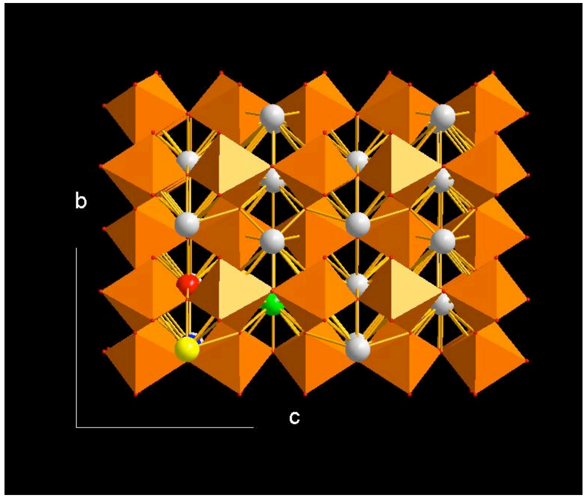

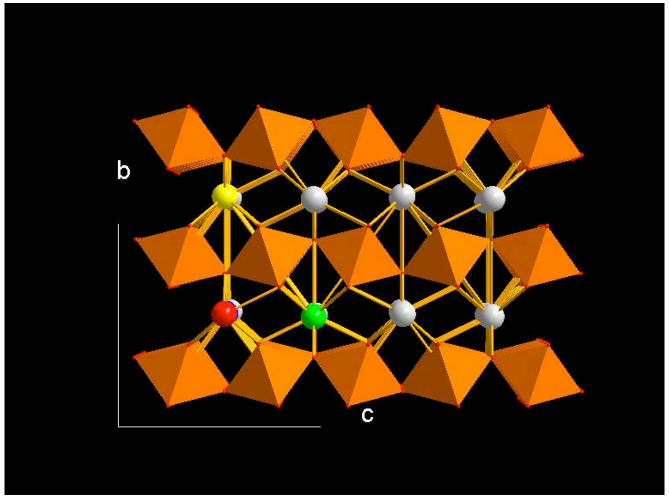

Gerd Steinle-Neumann[1]

Kanani K. M. Lee[1,2] , Mainak Mookherjee[1]
Sofia Akber-Knutson[3], David Dolejs[1,4]

[1]Bayerisches Geoinstitut, University of Bayreuth, Germany.
[2]Department of Geology and Geophysics, Yale University, New Haven, CT.
[3]Scripps Institution of Oceanography, UC San Diego, La Jolla, CA.
[4] Department of Petrology, Charles University, Prague, Czech Republic.

Potassium – why bother?

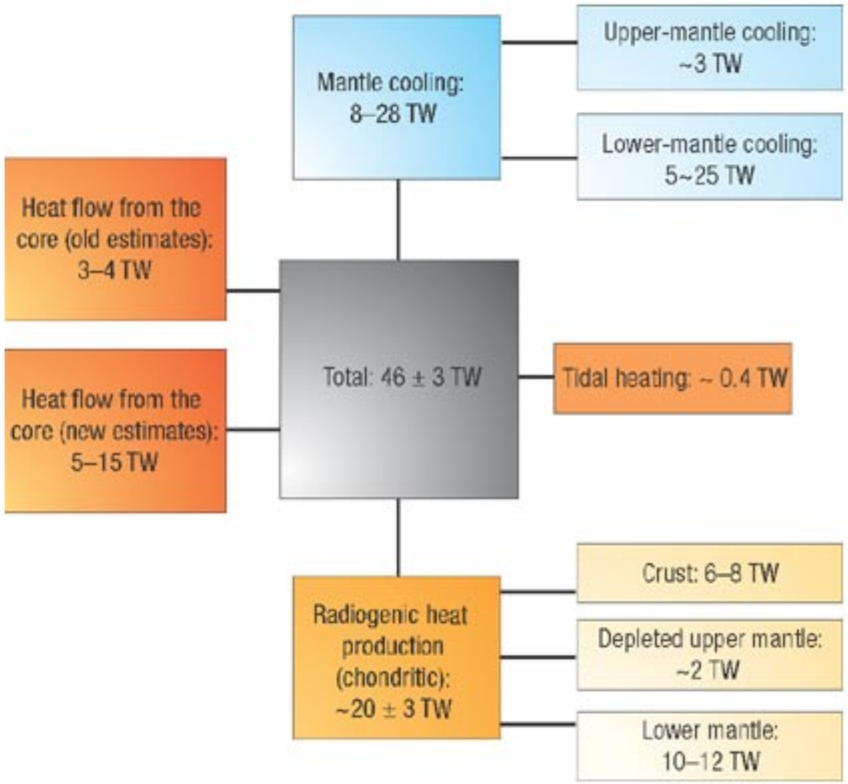

[Lay et al., 2008]

Heat budget of Earth

- secular cooling
- radiogenic heat production
- tidal heating

Radiogenic heat production (~20 TW):
- ^{235}U, ^{238}U, ^{232}Th, ^{40}K

Distribution of radiogenic isotopes critical for thermal state and evolution of Earth.
- known: fractionation into crust
- possible: reservoirs in the deep Earth
  - core
  - base of lower mantle/CMB
  - pockets of primitive reservoirs

Where is the potassium?

Model	MgO	FeO	CaO	Al_2O_3	SiO_2	Na_2O	K_2O
Pyrolite	49.8	6.2	2.9	2.2	38.7	0.1	0.02
Chondritic	53.2	7.7	3.9	1.0	34.2	0.6	0.07
MORB	14.9	7.1	13.9	10.2	51.8	2.1	0.1-0.5
Harzburgite	56.5	6.1	0.8	0.5	36.1	0	0
GLOSS	2.5	5.2	6.0	11.9	58.6	2.4	2.0

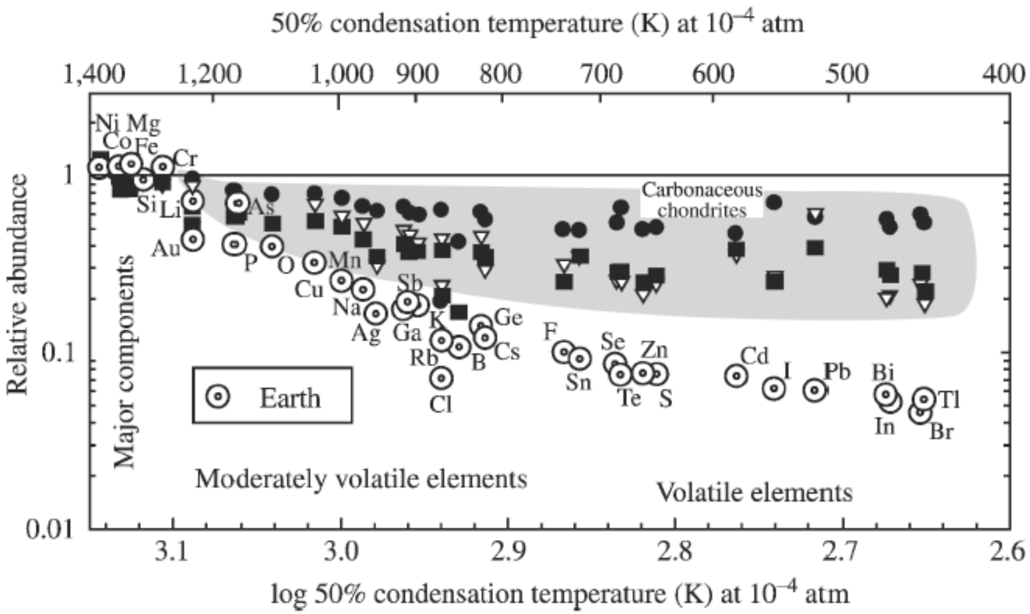

[McDonough, 2003]

Geochemistry of potassium

- moderately volatile: depletion during accretion
- lithophile at low pressure: silicate Earth @ differentiation
- high P behavior unclear: siderophile and/or chalcophile?

  [Lee et al., 2004; Murthy et al., 2003]

- LIL element: fractionation to basalt (MORB and OIB)

Where is the potassium?

Model	MgO	FeO	CaO	Al_2O_3	SiO_2	Na_2O	K_2O
Pyrolite	49.8	6.2	2.9	2.2	38.7	0.1	0.02
Chondritic	53.2	7.7	3.9	1.0	34.2	0.6	0.07
MORB	14.9	7.1	13.9	10.2	51.8	2.1	0.1-0.5
Harzburgite	56.5	6.1	0.8	0.5	36.1	0	0
GLOSS	2.5	5.2	6.0	11.9	58.6	2.4	2.0

1

2

Two questions

1. Distribution of K in the deep Earth aggregate chemistry:
   reservoirs in the deep mantle (D") or core?
   - K. K. M. Lee, S. Akber-Knutson, D. Dolejs
   Concentration of K *low*, separate phase unlikely to exist for aggregate mantle.

2. The role of K in the suducting slab:
   Can the elasticity of hollandite be used to detect deeply subducted crust?
   - M. Mookherjee

Significance of radiogenic heat production in the core

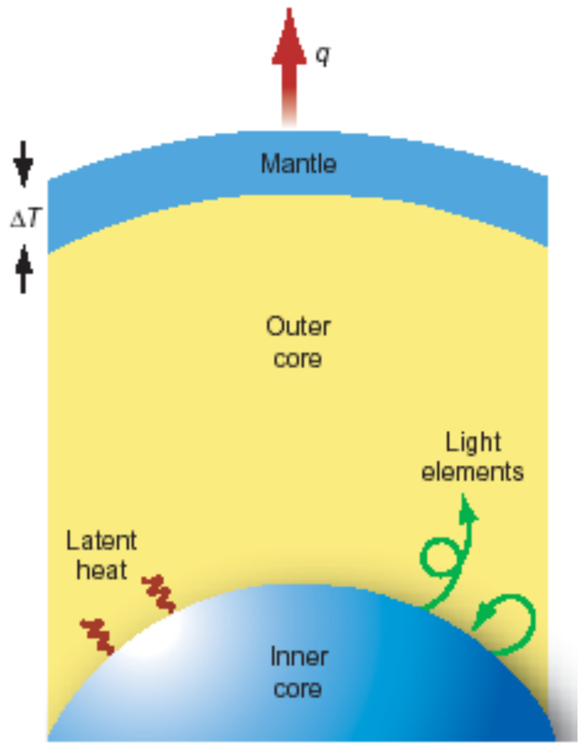

[Buffett, 2003]

Buoyancy forces powering the dynamo:

- Secular cooling
- Chemical buoyancy
- Latent heat release

IC age unlikely to exceed 1.5 Ga
Superheating of core before 2 Ga

[Buffett, 2003; Nimmo et al., 2004]

Solutions:

- Power requirements of the dynamo smaller than 1 TW [Christensen and Tilgner, 2004]
- Radioactive heat sources in the core
- Radioactive elements accumulated near CMB
- Thermal conductivity of core small

Possible reservoirs in the deep Earth

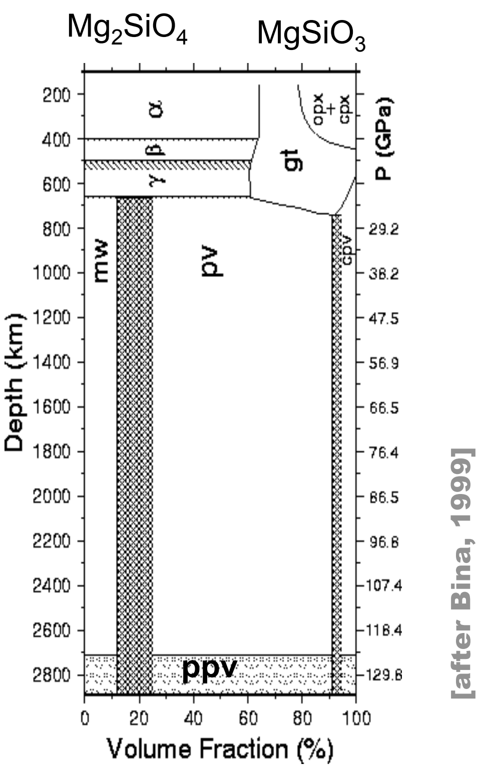

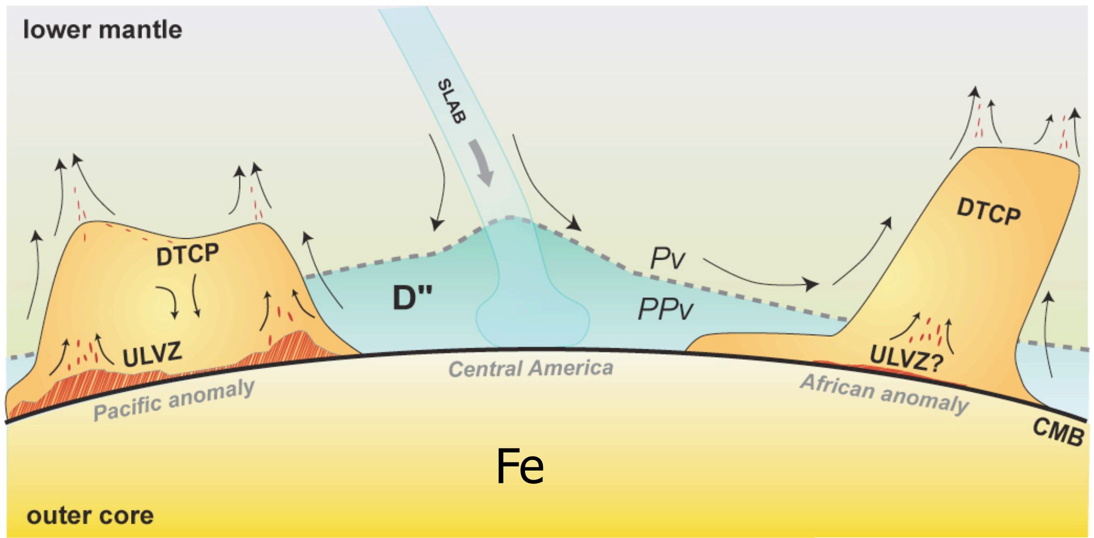

[Garnero et al., 2006]

Reservoir		**K (U/Th) partitioning**
➢ core		Fe - mantle silicates
➢ lower mantle: D″		pv - ppv (- Ca-pv - MgO)
DTCP	???	

Approach

Energetics of chemical reactions over wide pressure range

Lower mantle:
$(Mg_{30}\mathbf{M}K)Si_{32}O_{96}$ (pv) +32$MgSiO_3$ (ppv)↔$(Mg_{30}\mathbf{M}K)Si_{32}O_{96}$ (ppv) +32$MgSiO_3$ (pv),
with **M**=Fe,Al.

Core:
$(Mg_{30}FeK)Si_{32}O_{96}$ (pv) + A Fe ↔ $(Mg_{30}Fe_2)Si_{32}O_{96}$ (pv) + $Fe_{A-1}K$
with A=32, 48, 96.

$$K_D \equiv \exp\left(\frac{-\Delta G}{k_B T}\right) = \frac{\left(x_{K,pv}\right)\left(1 - x_{K,ppv}\right)}{\left(x_{K,ppv}\right)\left(1 - x_{K,pv}\right)}$$

Equilibrium constant

Energetics

$$K_D \equiv \exp\left(\frac{-\Delta G}{k_B T}\right) \qquad G(P,T)=E+PV-TS$$

- Internal energy *E(V)* from static ab-initio computation

  $(Mg_{30}\mathbf{M}K)Si_{32}O_{96}$ (pv/ppv) — **M**,K adjacent A sites
  with **M**=Fe, Al

  $(Mg_{30}Fe_2)Si_{32}O_{96}$ (pv/ppv) — Fe,Fe adjacent A sites [Stackhouse et al., 2006]
  $Fe_{A-1}K$, Fe_A — A atom SC
  with A=32, 48, 96, (144, 196).

- Computational details:
  GGA, spin polarized, PAW, E_c=1000eV
  k-points such that convergence of E ~1meV
  Vienna *ab-initio* simulation package

Energetics

$$K_D \equiv \exp\left(\frac{-\Delta G}{k_B T}\right)$$

$G(P,T)=E+PV-TS$

- Internal energy $E(V)$ from static ab-initio computation
- PV from cold equation of state
- $S=S_{vib}+S_{mix}$

S_{mix} for Fe - silicate partitioning
S_{mix} cancels for pv-ppv due to arrangements

Arrangement issues

$$K_D \equiv \exp\left(\frac{-\Delta G}{k_B T}\right) \qquad G(P,T)=E+PV-TS$$

- Internal energy *E(V)* from static ab-initio computation

$(Mg_{30}\mathbf{M}K)Si_{32}O_{96}$ (pv/ppv) **M**,K adjacent A sites

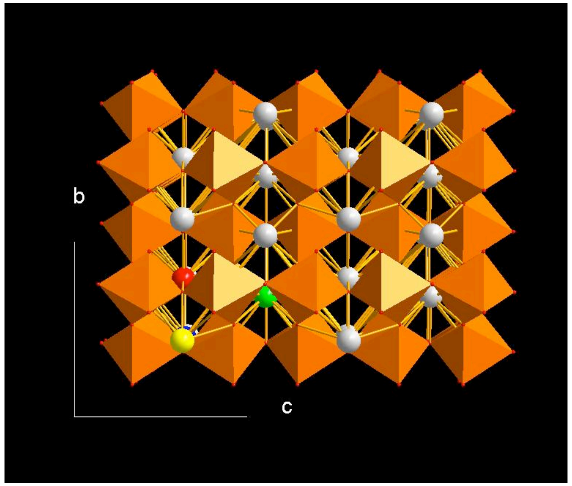

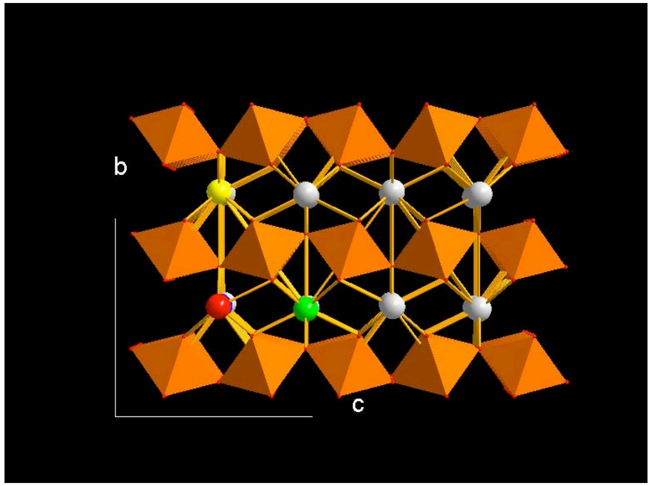

ΔE <1meV, within convergence criterion

Lower mantle partitioning

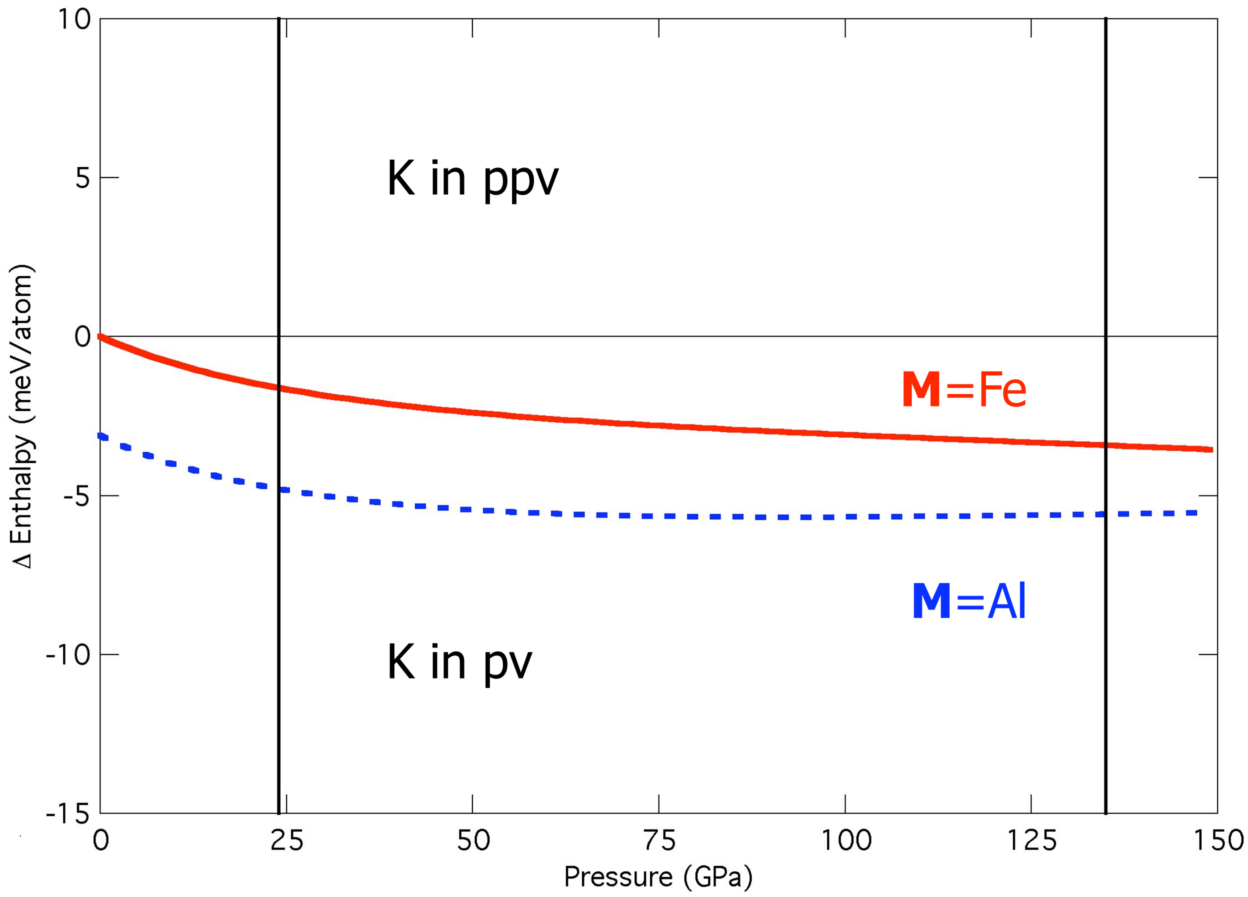

Lower mantle partitioning

P (GPa)	K_D $(Mg_{30}FeK)Si_{32}O_{96}$ at 3000 K	K_D $(Mg_{30}FeK)Si_{32}O_{96}$ at 5000 K	K_D $(Mg_{30}AlK)Si_{32}O_{96}$ at 3000 K	K_D $(Mg_{30}AlK)Si_{32}O_{96}$ at 5000 K
100	6.8	3.1	33.5	8.2
110	7.2	3.3	33.2	8.2
120	7.6	3.4	32.7	8.1
130	8.1	3.5	31.1	8.0

Caveats

- other incorporation mechanisms: K**M**□↔MgSiO, …
- other phases (later)

Core partitioning

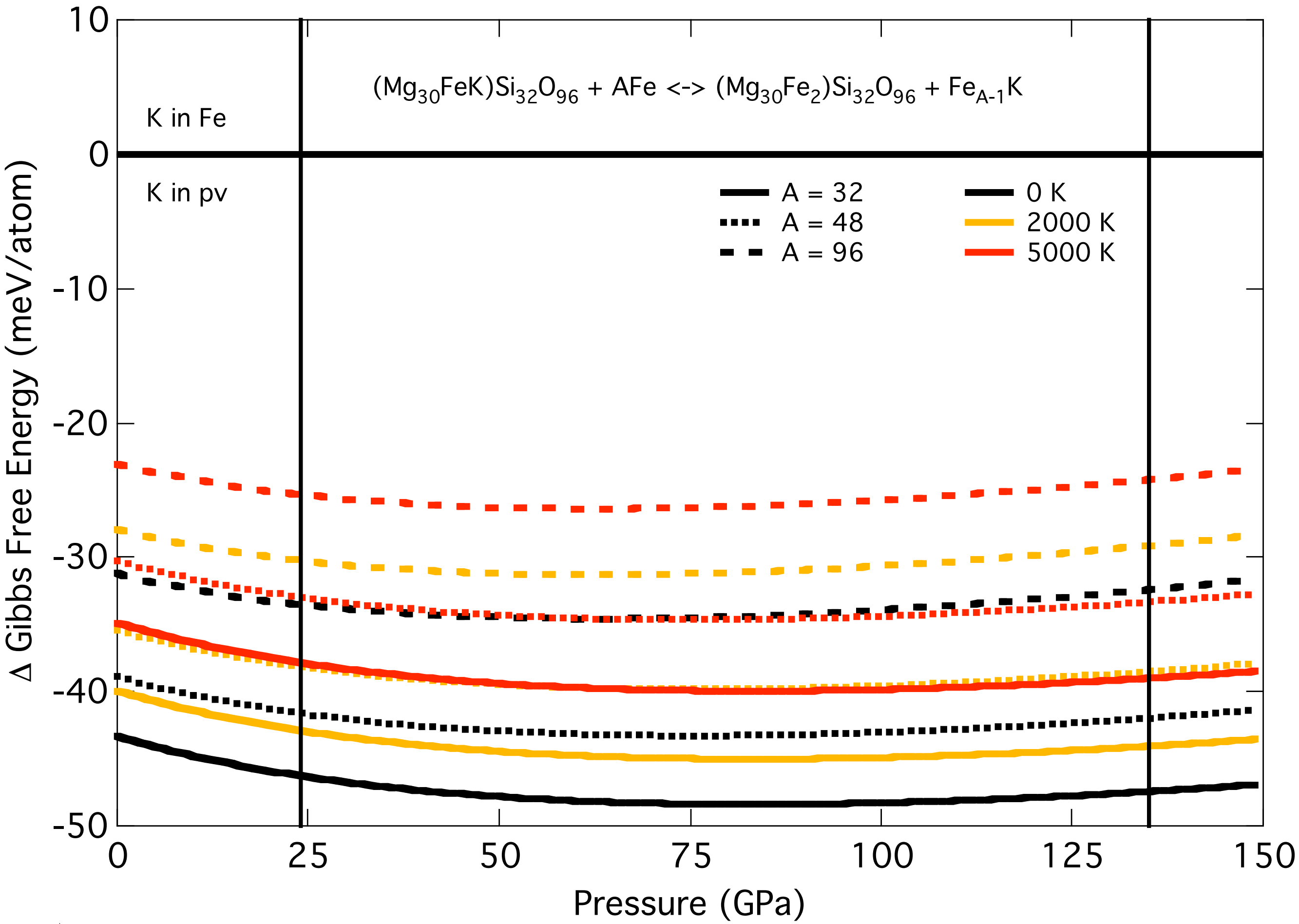

$K_D < 10^{-6}$ at CMB conditions

Conclusions - core partitioning

- partitioning of K between Fe-bearing $MgSiO_3$ perovskite and Fe is near zero (static computations)

Caveats

- S_{vib}
- Fe melt (entropy)
- role of light element (O, S, Si)

[Murthy et al., 200 3; Gessmann and Wood, 2002]

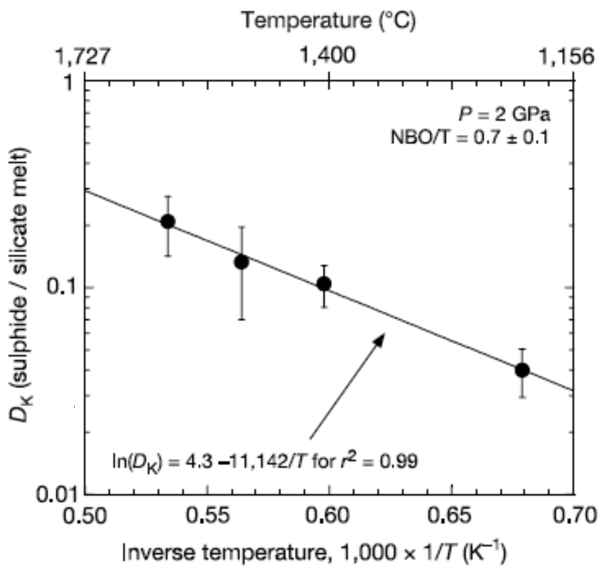

[Murthy et al., 2003]

Potassium in the lower mantle - what phase then?

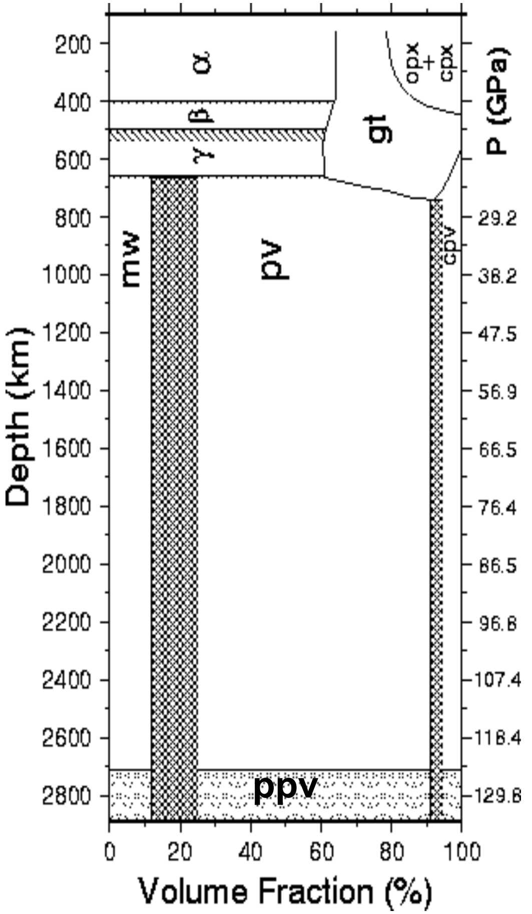

[after Bina, 1999]

- Three reactions forming AlK-bearing phases from the oxides:

$$30CaSiO_3 + 1/2Al_2O_3 + 1/2K_2O + 2SiO_2 \leftrightarrow (Ca_{30}AlK)Si_{32}O_{96}$$

$$30MgSiO_3 + 1/2Al_2O_3 + 1/2K_2O + 2SiO_2 \leftrightarrow (Mg_{30}AlK)Si_{32}O_{96}$$

$$30MgO + 1/2Al_2O_3 + 1/2K_2O \leftrightarrow (Mg_{30}AlK)O_{32}$$

- Al_2O_3 in the corundum structure (doesn't matter)
- SiO_2 in the $CaCl_2$ structure

- Experimental picture:
  - K in Ca-pv based on crystal chemistry [Kesson et al., 1998]
  - K in mw from microprobe analysis [Tronnes and Frost, 2002]

[Murakami et al., 2005]

Potassium in the lower mantle - what phase then?

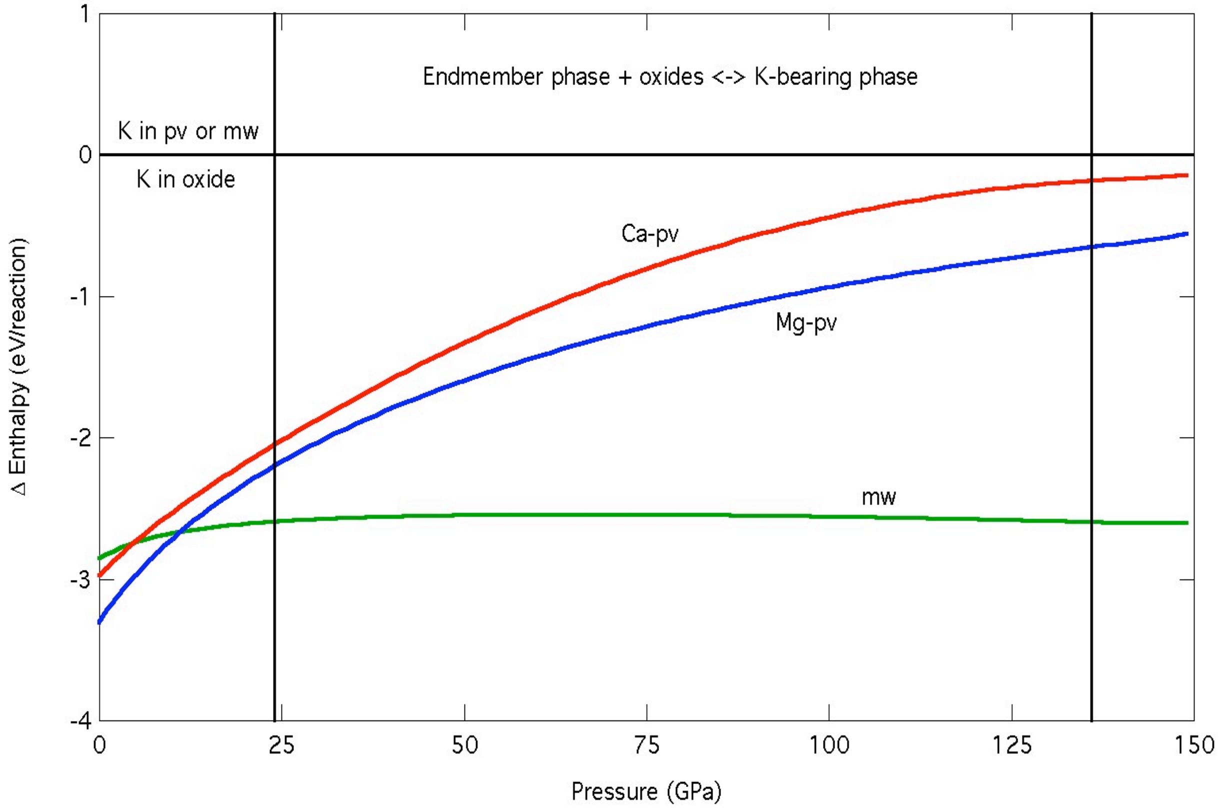

- Adding entropy will push curves up
- Potassium prefers Ca-pv over Mg-pv and mw

Conclusion - partitioning

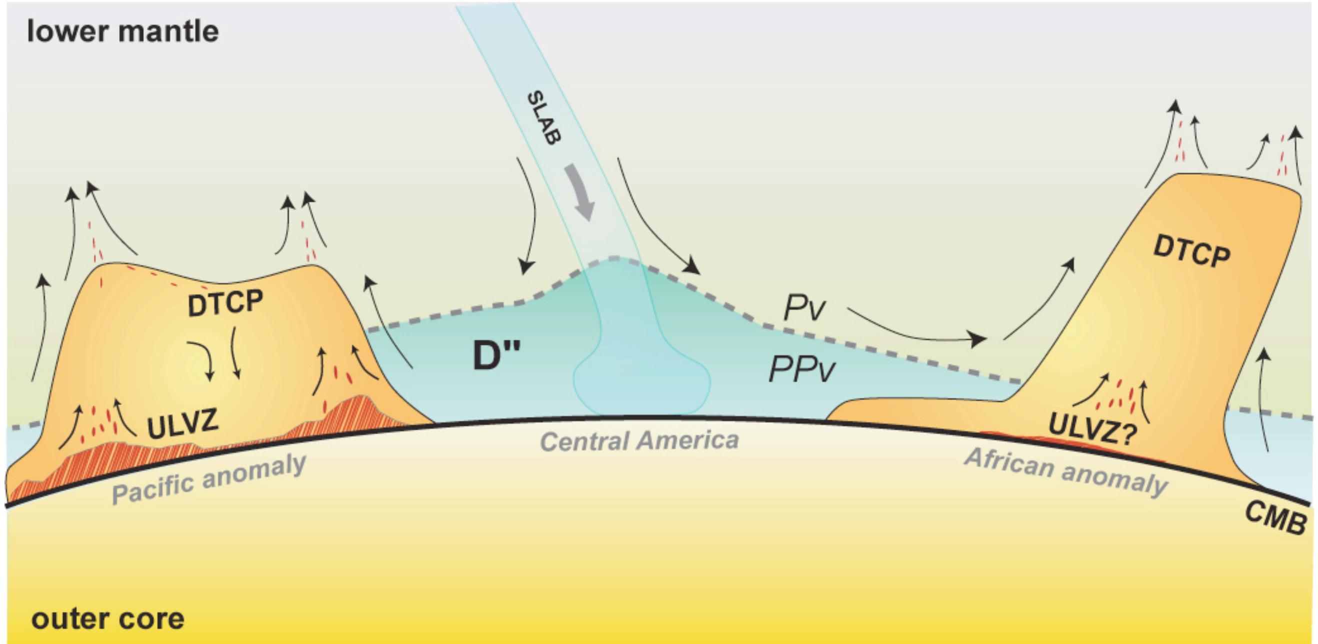

[Garnero et al., 2006]

➢ global deep Earth reservoirs for K unlikely to exist:
- core
- D″

➢ K prefers to partition into Ca-pv in the LM phase assemblage (preliminary results)

Conclusions - core partitioning

- partitioning of K between Fe-bearing $MgSiO_3$ perovskite and Fe is near zero (static computations)

Caveats

- S_{vib}
- Fe melt (entropy)
- role of light element (O, S, Si)

[Murthy et al., 200 3; Gessmann and Wood, 2002]

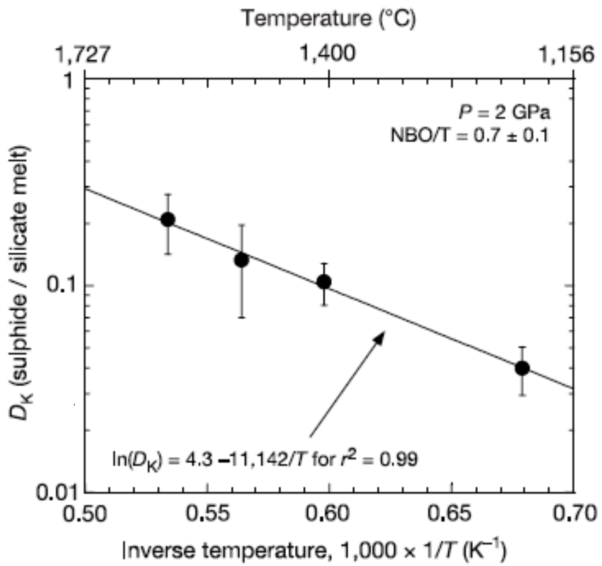

[Murthy et al., 2003]

Where is the potassium?

Model	MgO	FeO	CaO	Al_2O_3	SiO_2	Na_2O	K_2O
Pyrolite	49.8	6.2	2.9	2.2	38.7	0.1	0.02
Chondritic	53.2	7.7	3.9	1.0	34.2	0.6	0.07
MORB	14.9	7.1	13.9	10.2	51.8	2.1	0.1-0.5
Harzburgite	56.5	6.1	0.8	0.5	36.1	0	0
GLOSS	2.5	5.2	6.0	11.9	58.6	2.4	2.0

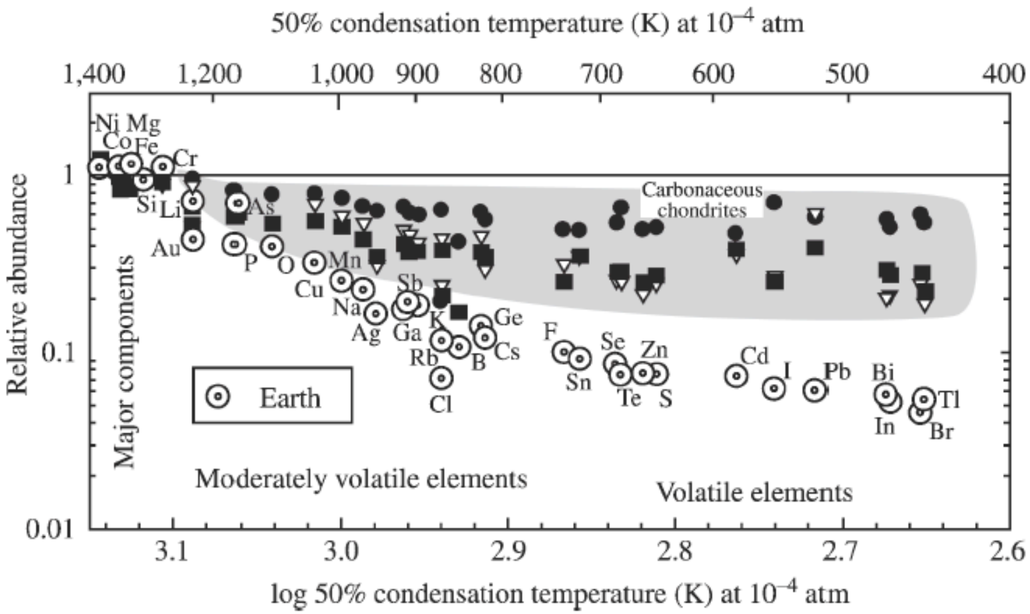

[McDonough, 2003]

Geochemistry of potassium

- moderately volatile: depletion during accretion
- lithophile at low pressure: silicate Earth @ differentiation
- high P behavior unclear: siderophile and/or chalcophile?

[Lee et al., 2004; Murthy et al., 2003]

- LIL element: fractionation to basalt (MORB and OIB)

Geochemical evidence of subducted sediments and crust

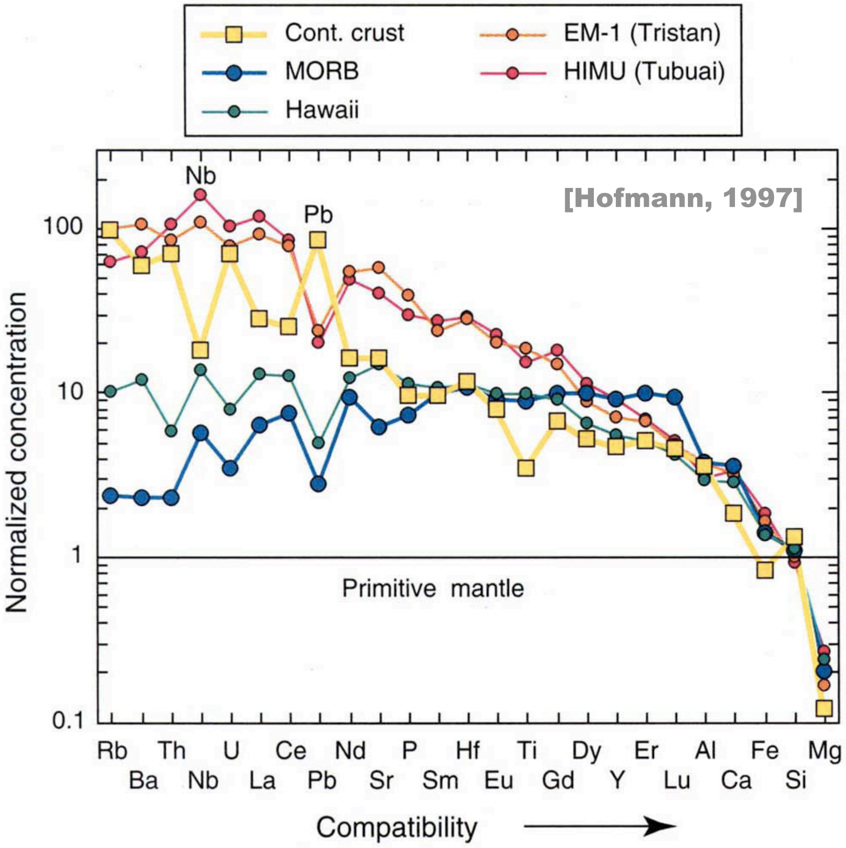

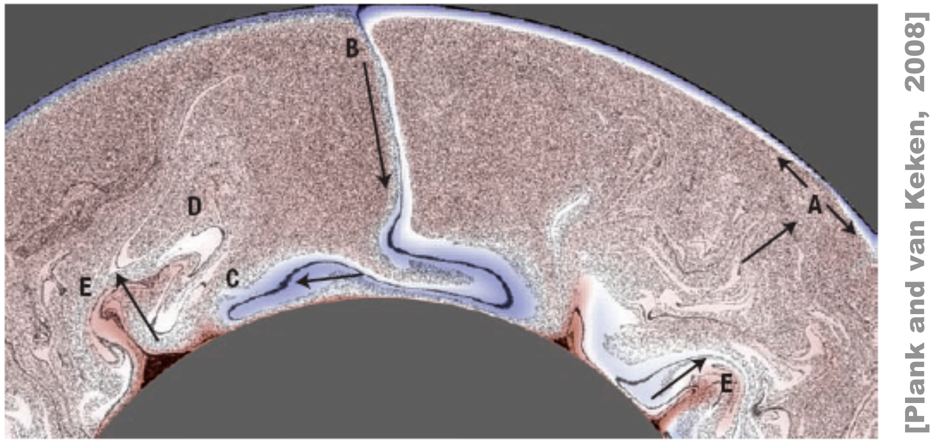

- OIB enriched in imcompatible elements (LIL)
- deep enriched reservoirs in TZ and LM
- possible source: subducted sediments or crust

Phase relations

terrigeneous sediments

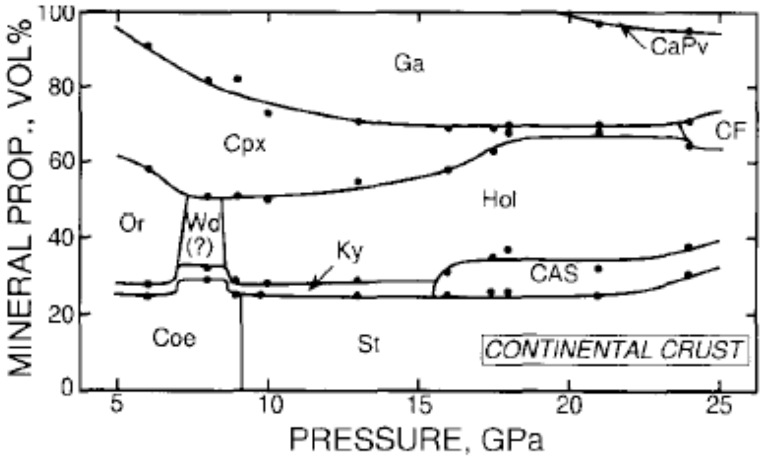

pelagic sediments

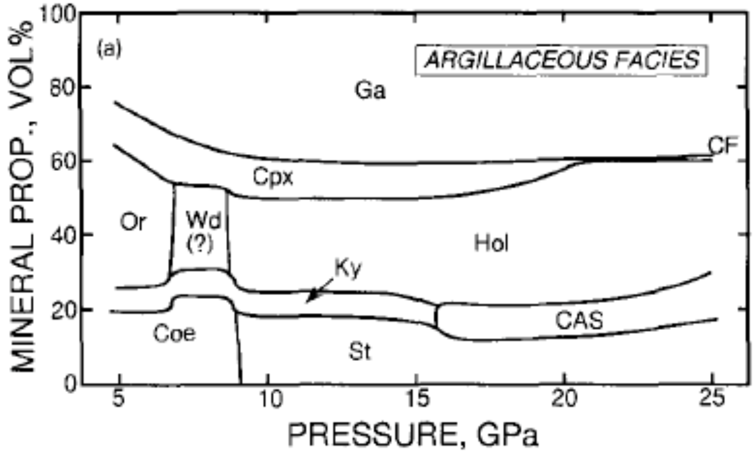

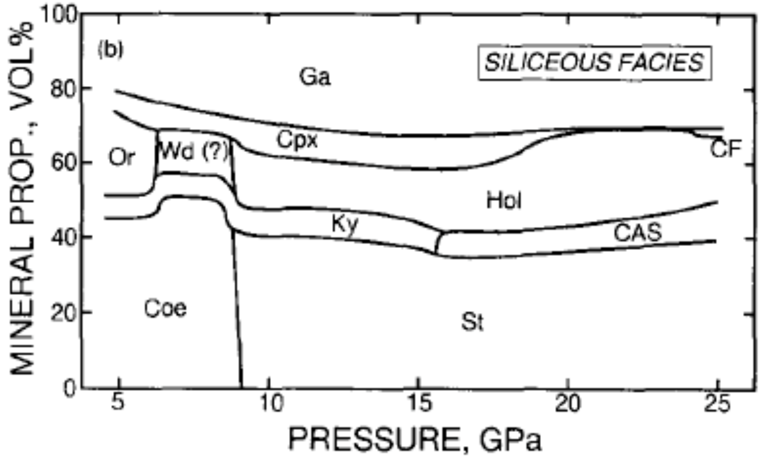

[Irifune and Ringwood, 1994]

- hollandite important component of subducted sediments
- even for enriched MORB hollandite liquidus phase [Wang and Takahashi, 1999]
- K-hollandite found in diamond inclusions from LM [Stachel et al., 2000]

Hollandite

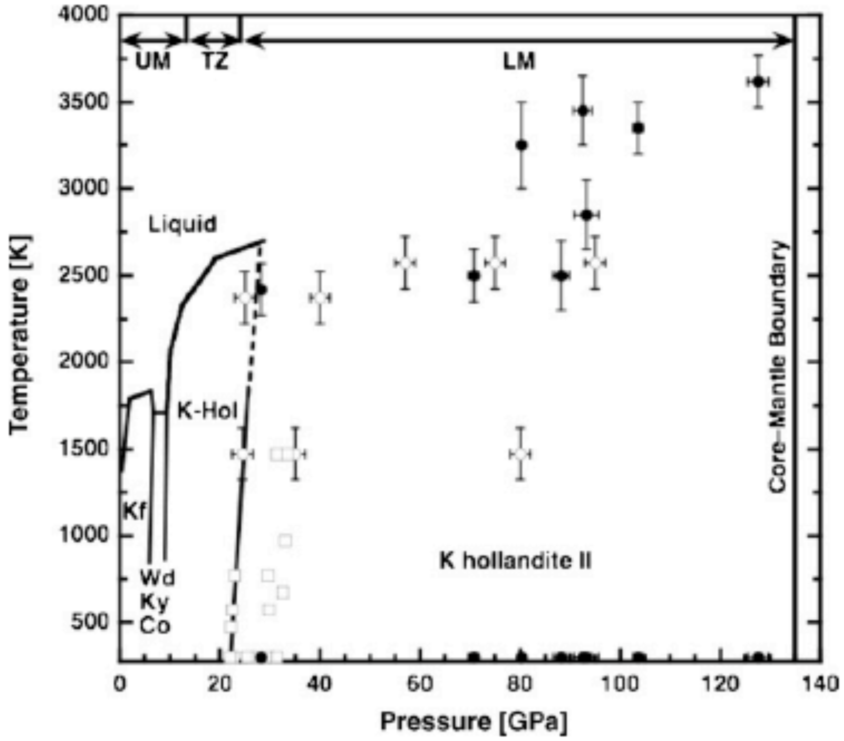

[Hirao et al., 2006]

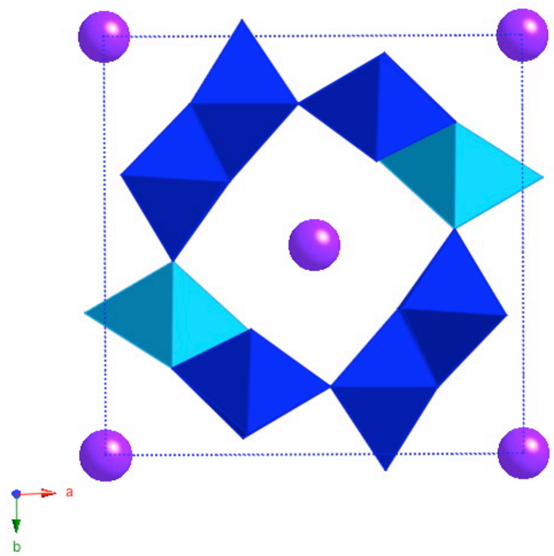

- K-hollandite $KAlSi_3O_8$ as model hollandite
- phase transition from tetragonal to monoclinic at ~20 GPa

- phase transition depends on temperature and chemistry

More geochemistry

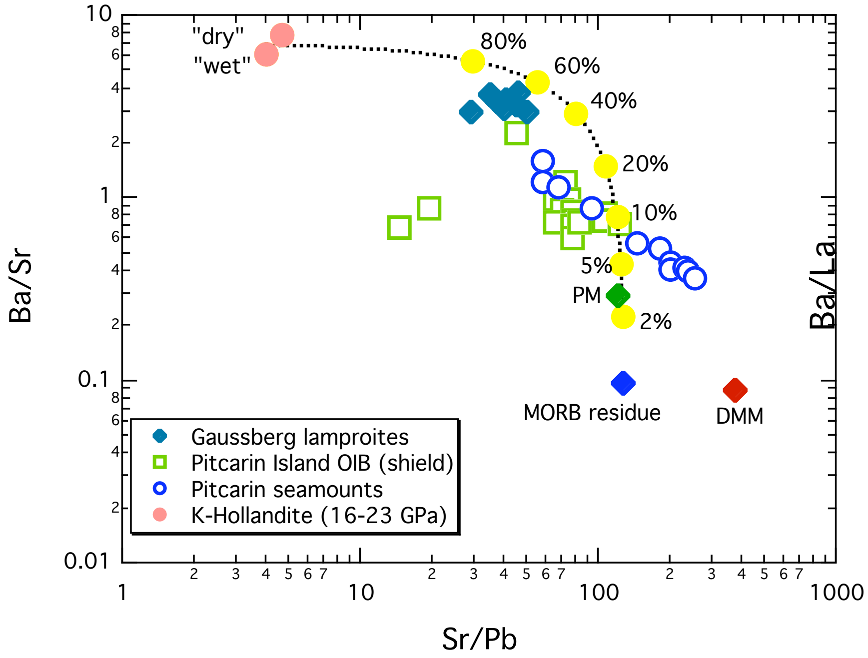

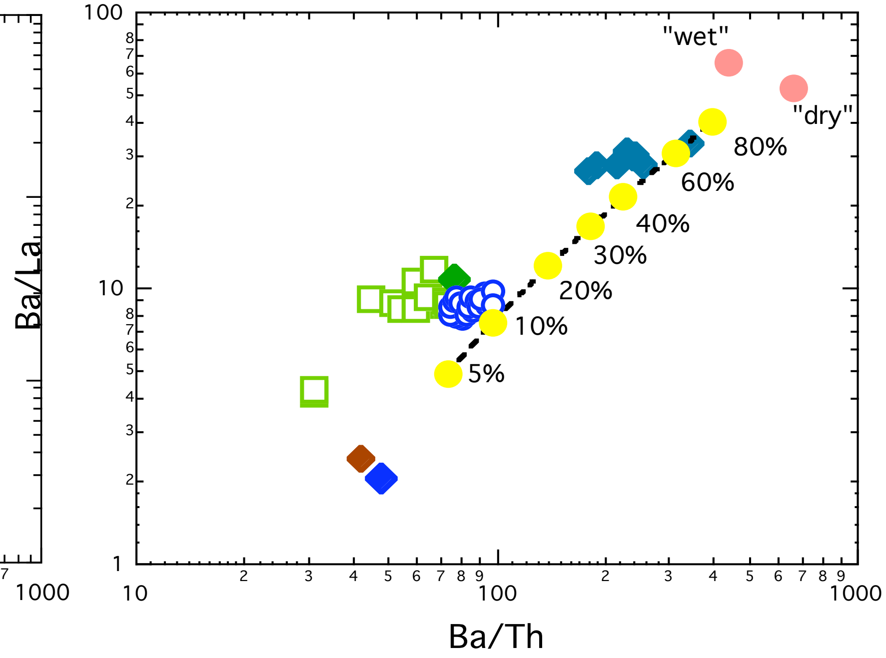

[Rapp et al., 2008]

➢ trace element budget for OIB from sediments:
- 10% Pitcairn
- 40% Gaussberg Lamprotites (Antarctica)

Some seismology

[Li et al., 2008]

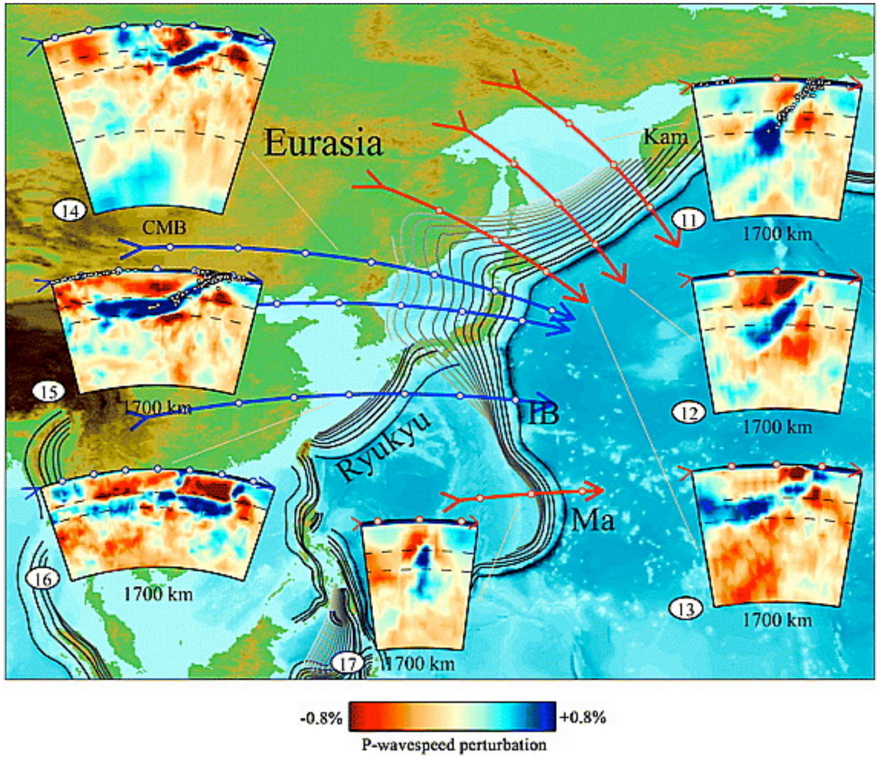

- ➢ transition pressure ~20 GPa
- ➢ elastic signature of transition?

- ➢ slabs in TZ or uppermost LM
- ➢ stagnant slabs particularly interesting

Birch's law

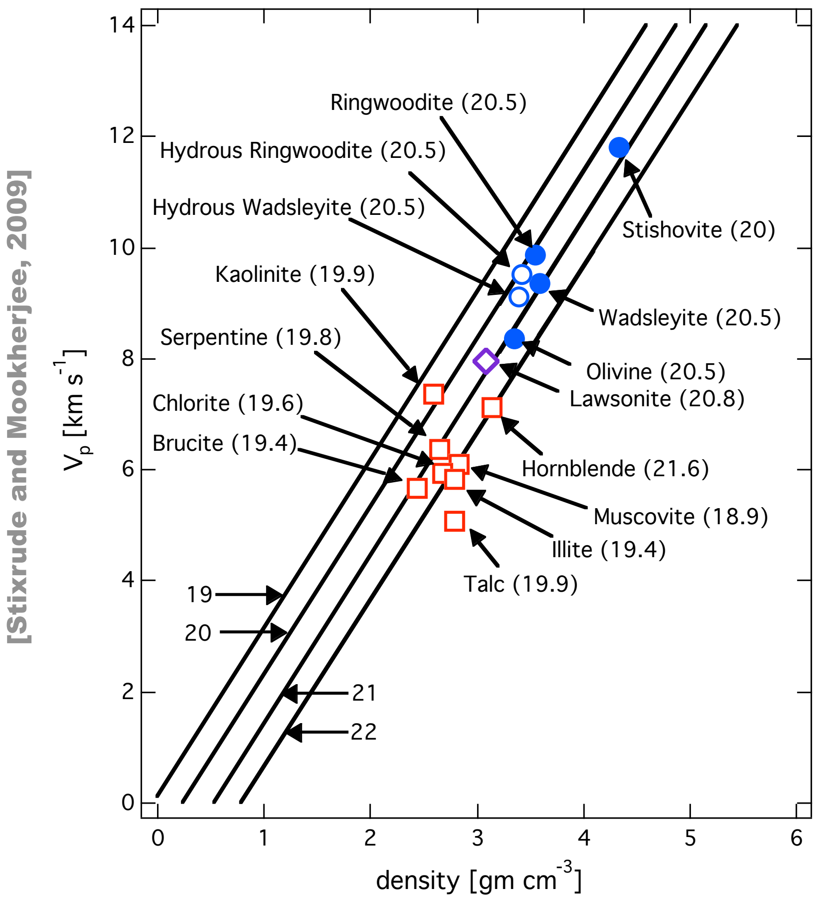

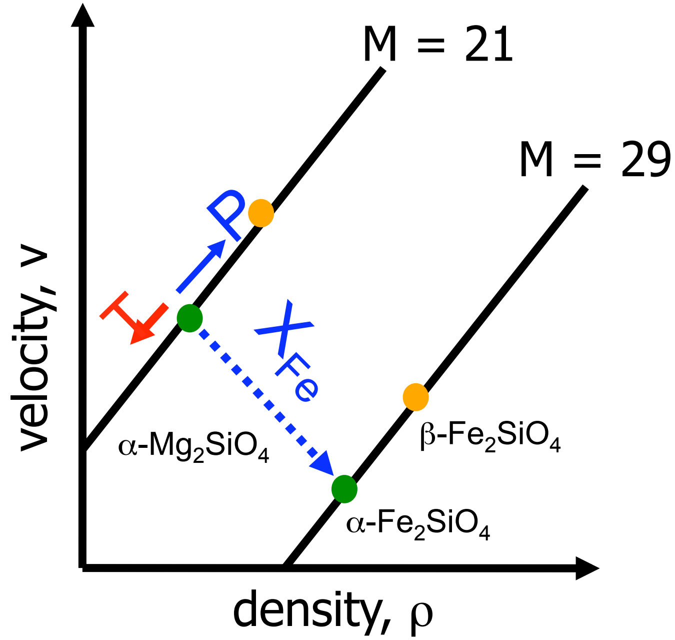

- map heterogeneity by velocity anomaly

Computations

- DFT based computations
- Vienna ab-initio simulation package
- norm-conserving pseudopotentials
- 1x1x4 supercell (104 atoms)
- Γ-point, E_{cut}=400 eV
- tetagonal and monoclinic phases of K-hollandite
- static computations + thermal corrections
- E-V equation-of-state
- Elasticity from stress-strain coefficients

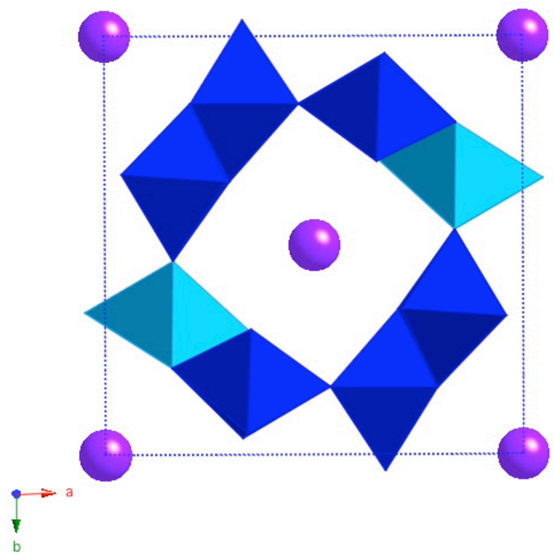

- K-hollandite $KAlSi_3O_8$ as model hollandite
- here SiO_6 and AlO_6 octahera ordered

Phase transition

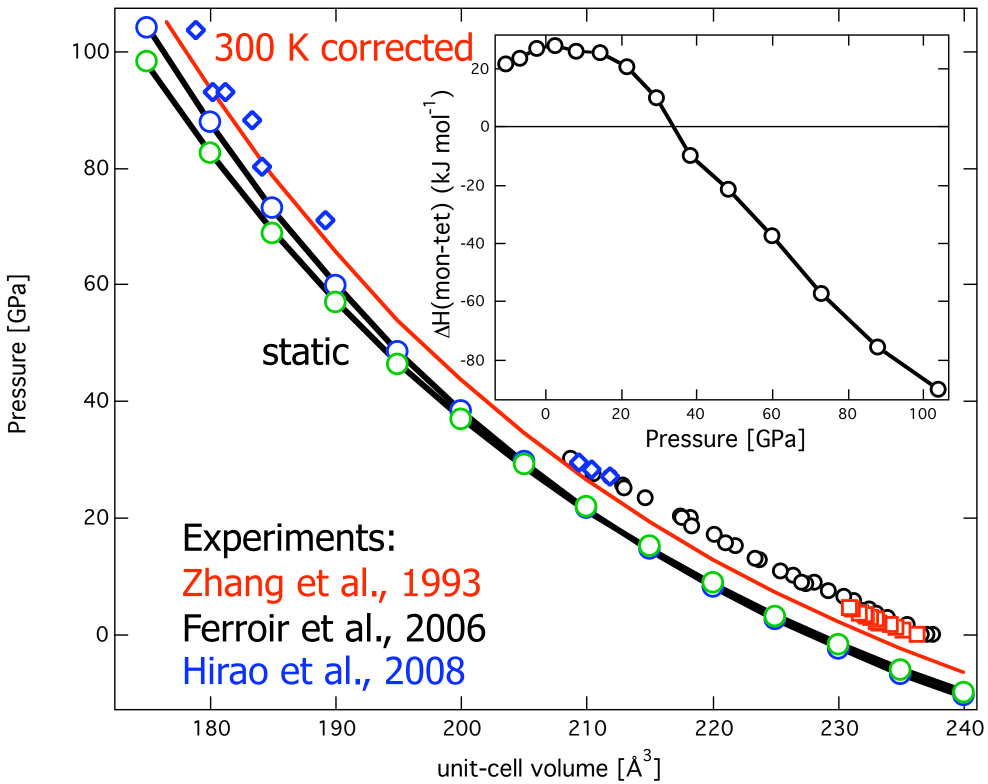

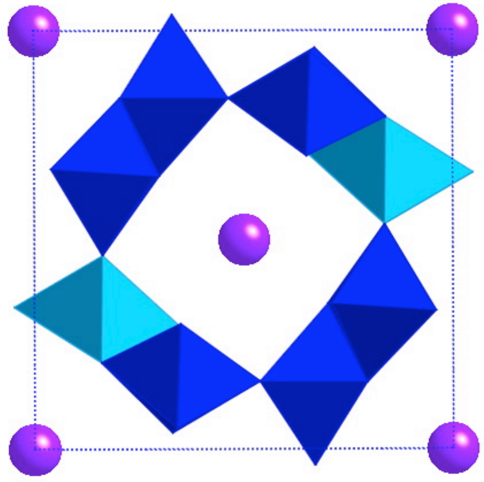

	V_0 (Å^3)	K_0 (GPa)	K'_0
theory (this study)			
hollandite I (static)	227.65	225.0	4.3
hollandite I (300 K)	232.23	212.0	4.3
hollandite I I	228.02	220.5	3.9
hollandite II (300 K)	234.95	207.7	3.9
Experiments			
	241.06[1]		
	236.73[2]		
hollandite I	236.26[3]	180.0	4.0
	237.60[4]	183.0	4.0
	237.01[5]	201.4	4.0
hollandite I I	232.30[6a]	232.0	4.0
	237.01[6b]	181.0	4.9

- phase transition predicted at ~30 GPa

Phase transition

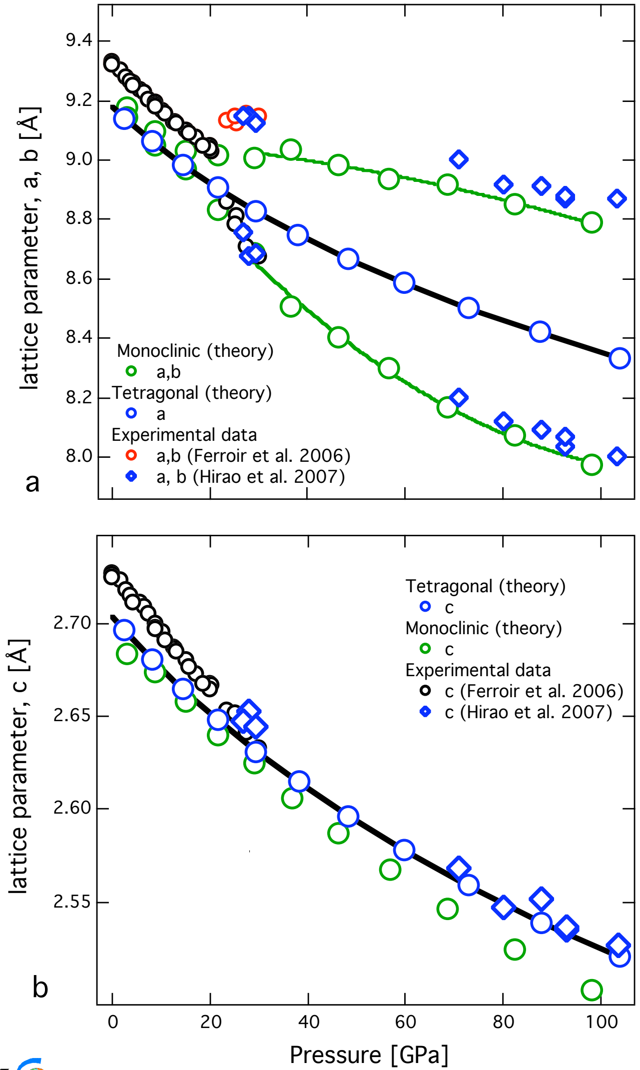

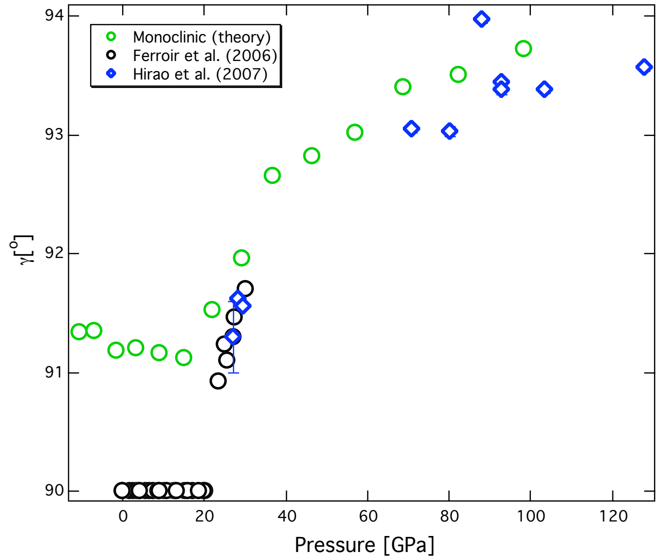

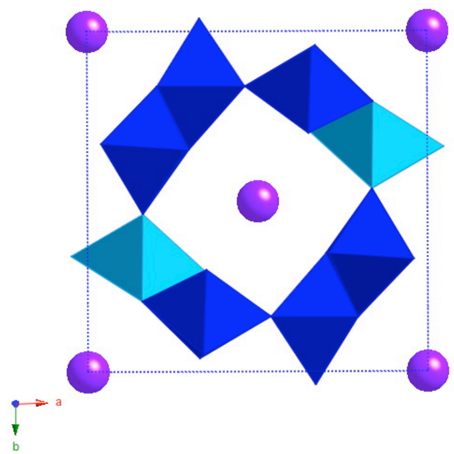

Phase transition

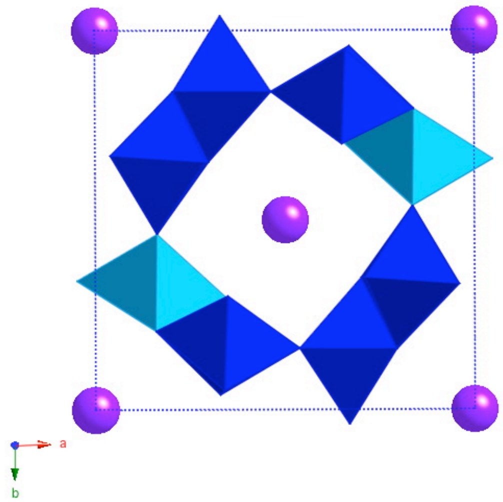

tetragonal phase
V = 210 Å^3, P~ 20 GPa

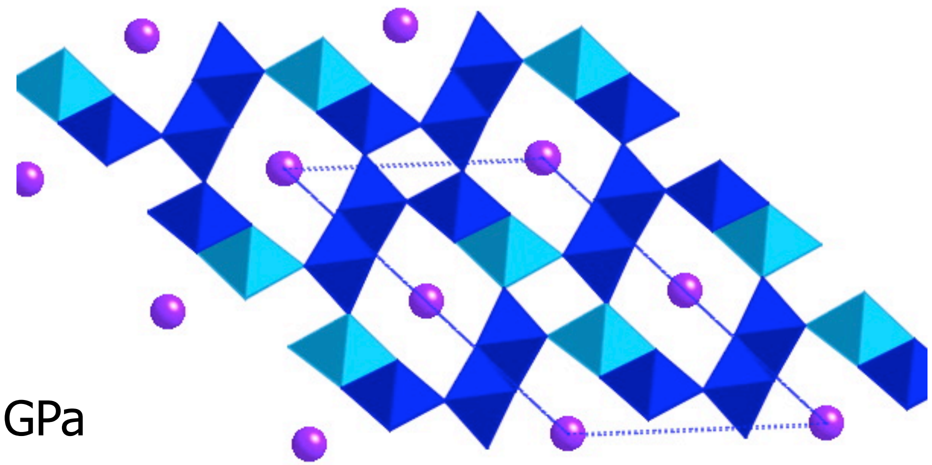

monoclinic phase
V= 175 Å^3, P ~ 100 GPa

Elasticity

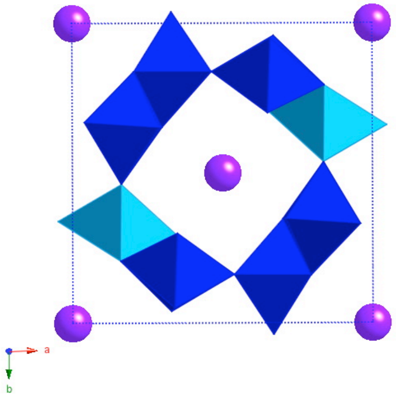

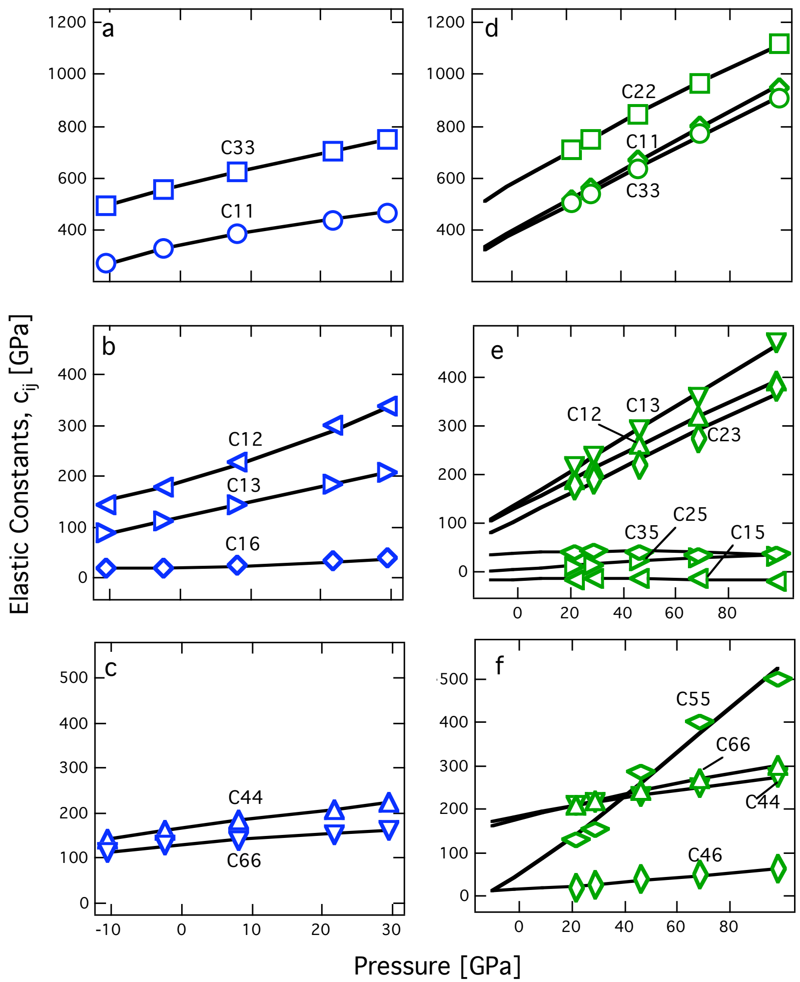
a
C33
C11
b
C12
C13
C16
c
C44
C66
d
C22
C11
C33
e
C12
C13
C23
C35
C25
C15
f
C55
C66
C44
C46
Elastic Constants, c_{ij} [GPa]
Pressure [GPa]

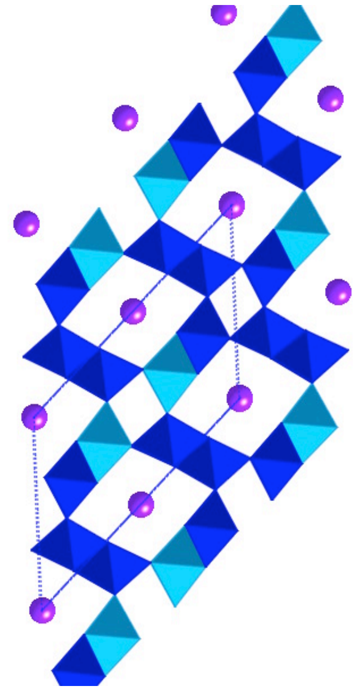

Map heterogeneity?

$V = a + b\rho$
$b = \text{constant}$
$a = f(M)$

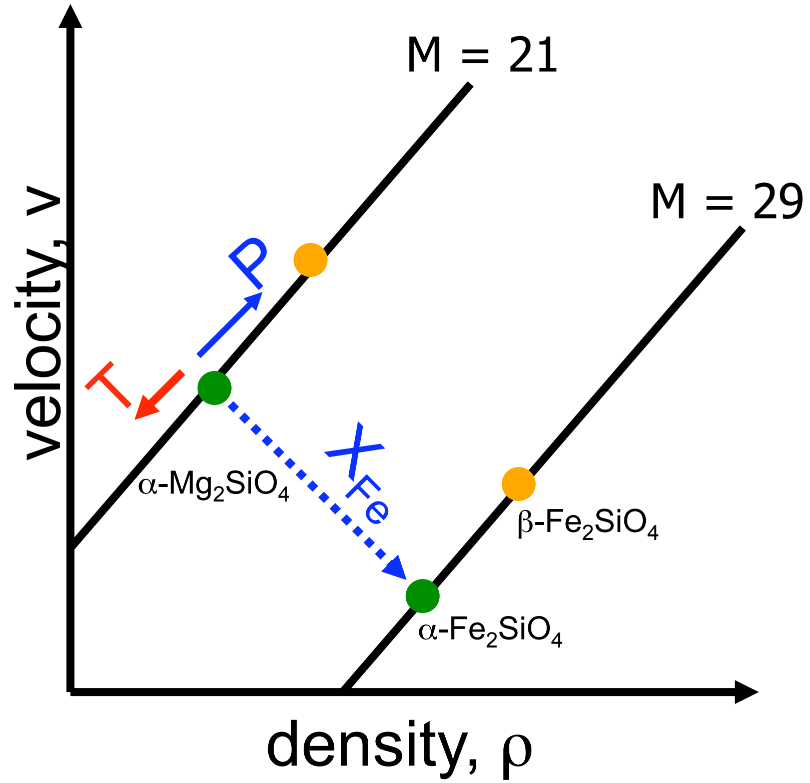

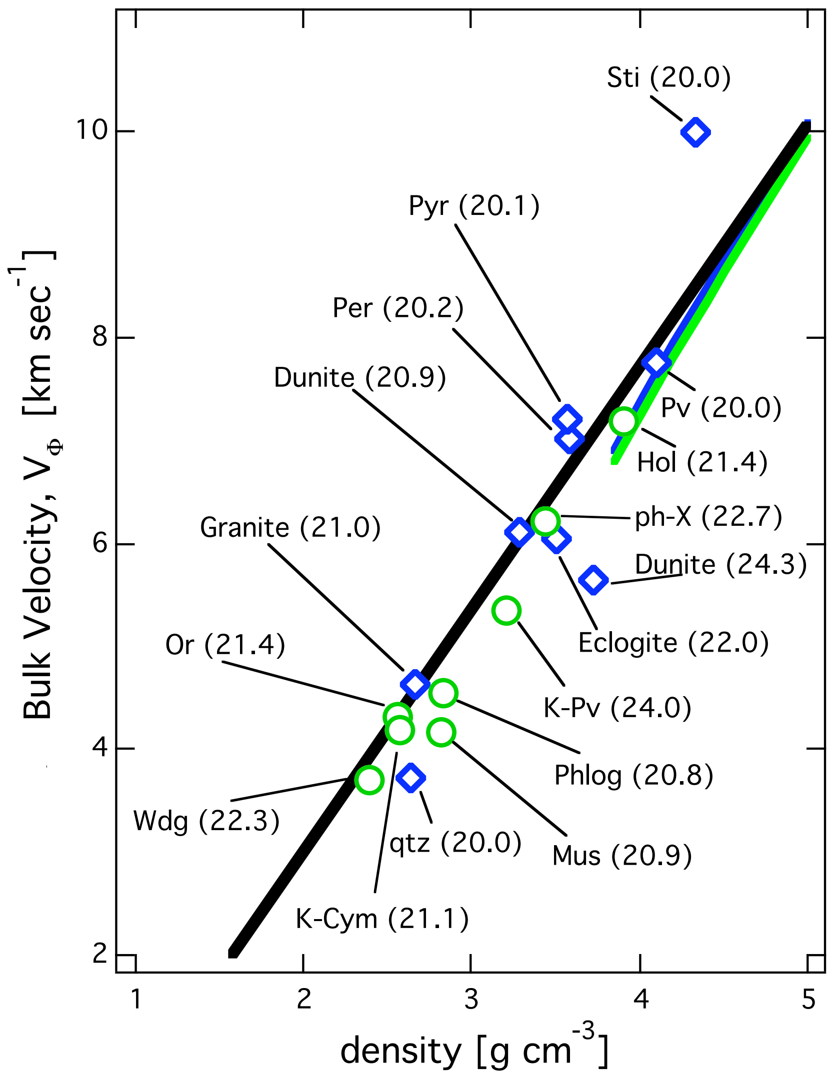

Aggregate seismic velocities

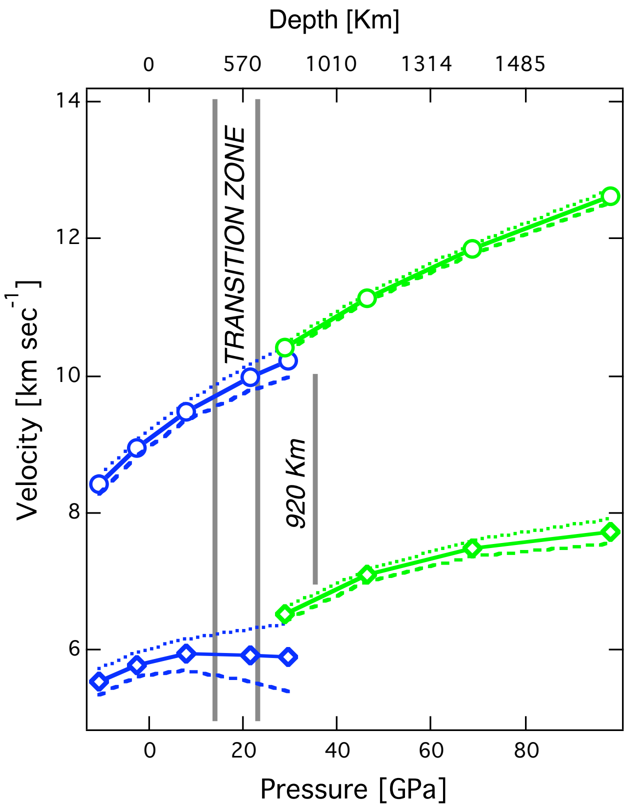

- phase transition predicted at ~30 GPa
- strong increase in v_S
- can cause scatter and reflections (920 km)

[Kawakatsu and Niu, 1994; Kaneshima and Helffrich, 1999; 2003]

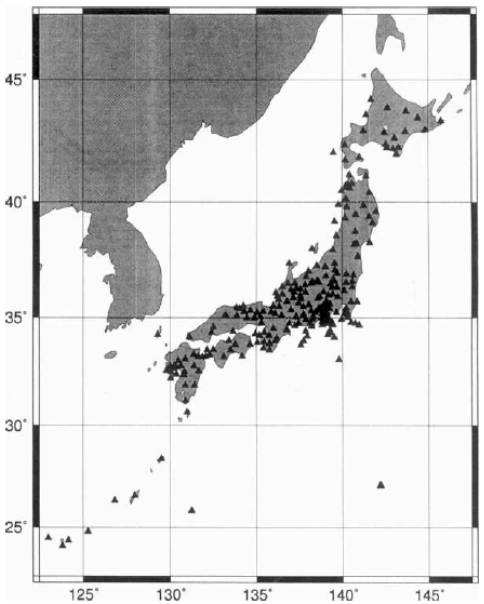

[Kawakatsu and Niu, 1994]

Aggregate seismic velocities

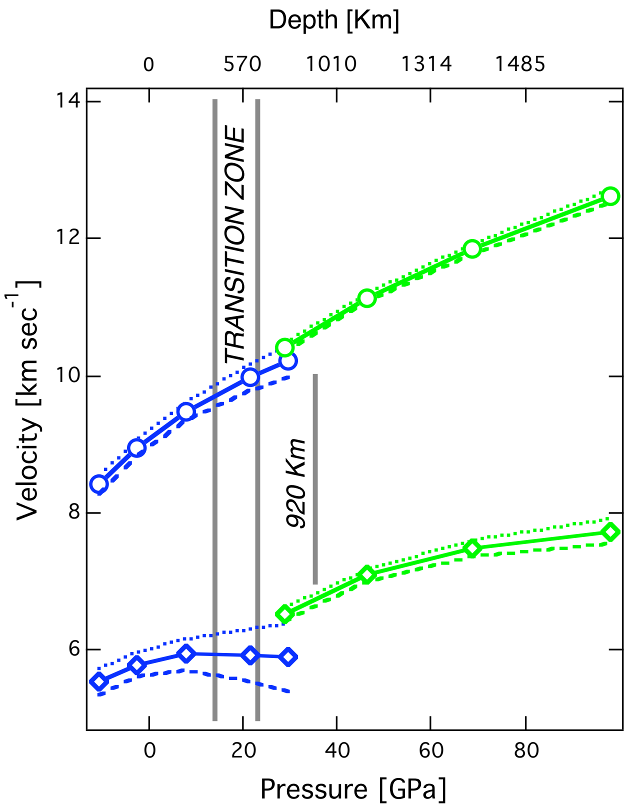

- phase transition predicted at ~30 GPa
- strong increase in v_S
- can cause scatter and reflections (920 km)

[Kawakatsu and Niu, 1994; Kaneshima and Helffrich, 1999; 2003]

- reflection coefficient

$$R_v = (\rho_{II} v_{II} - \rho_I v_I) / (\rho_{II} v_{II} + \rho_I v_I)$$

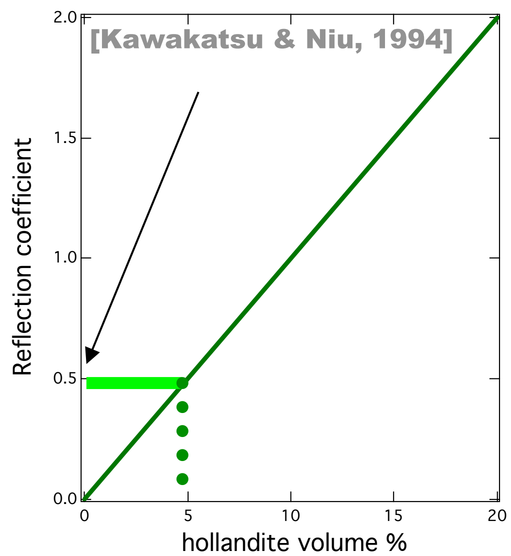

Seismology vs. geochemistry

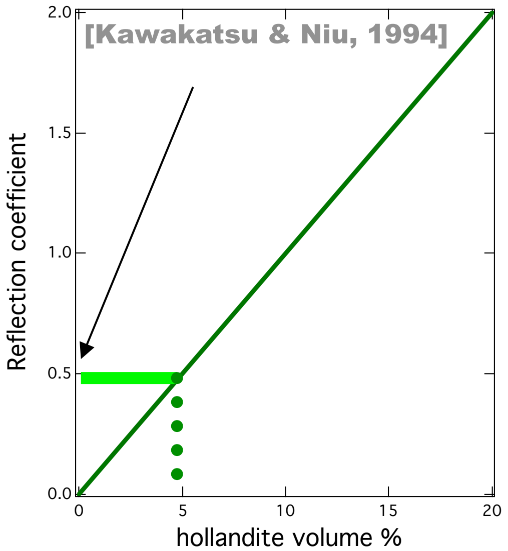

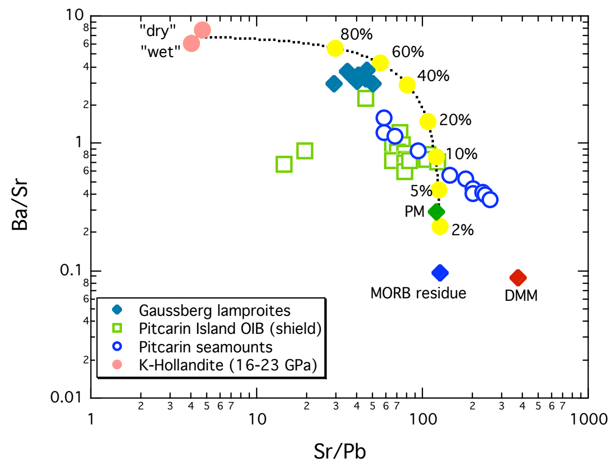

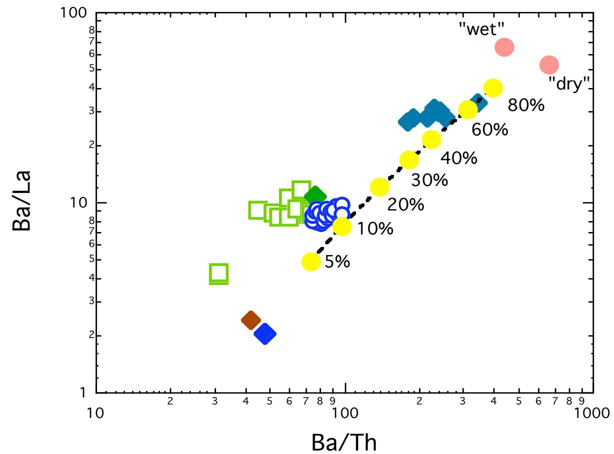

[Rapp et al., 2009]

Mid-mantle anisotropy

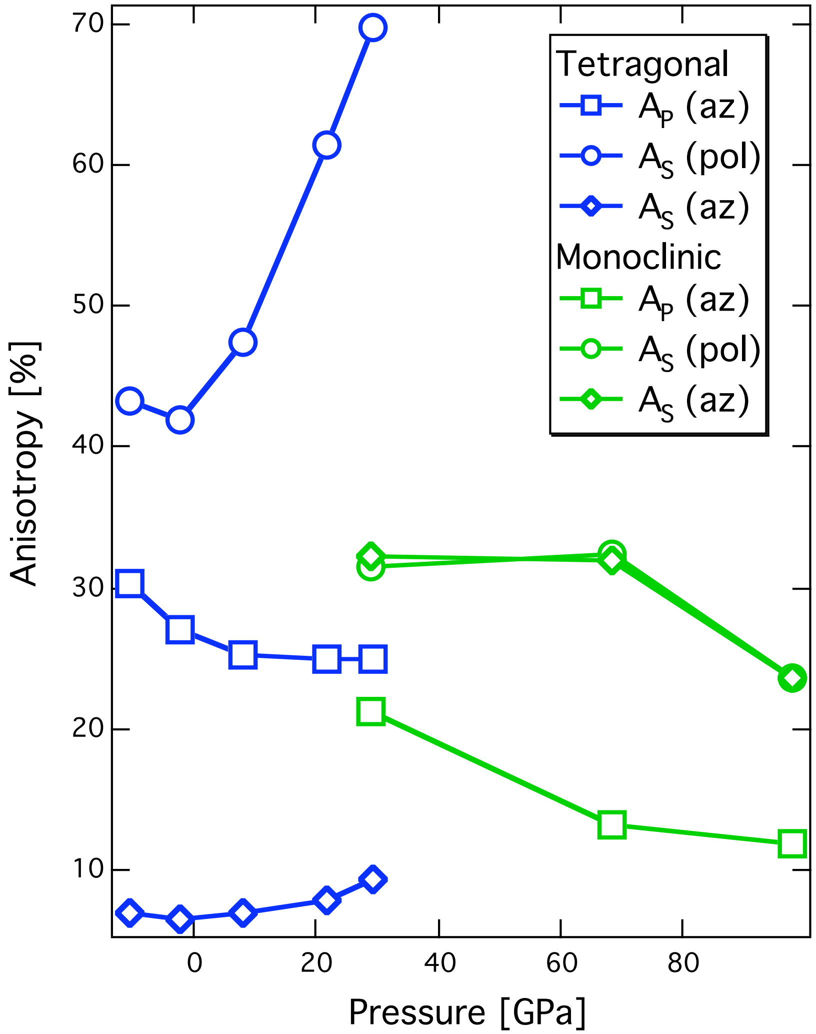

- strong anisotropy near transition
- mid-mantle anistropy, e.g. Tonga and New Hebridies

[Wookey et al., 2002; 2004; Heintz, 2006]

- possibly created through strong deviatoric stress

[Nipress et al., 2004]

- further work needed on plastic deformation

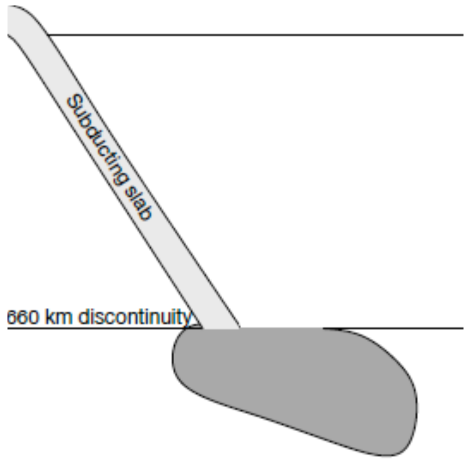

[Wookey et al., 2002]

Conclusions - hollandite

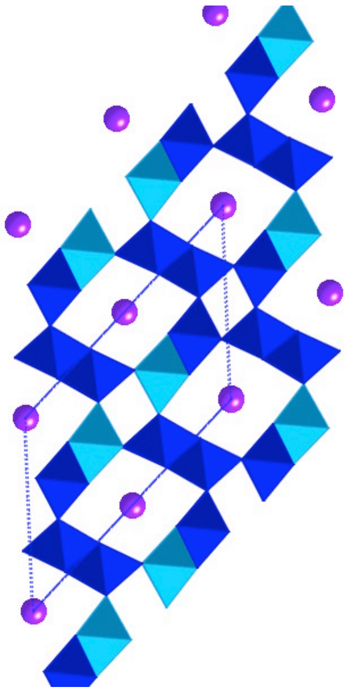

- Computations show good agreement in crystal-chemistry with experiments, including the tetragonal to monoclinic phase transition
- strong discontinuity in v_S predicted across phase transition, transition might be related to 920 km discontinuity observed in some subduction zones
- hollandite is strongly anisotropic, and mid-mantle anisotropy could be related to it